Characterization of Wall Film Formation from Impinging Diesel Fuel Sprays using LIF

A. Magnusson*, M. Begliatti, F. Borja Hervás and M. Andersson
Department of Applied Mechanics
Chalmers University of Technology
Göteborg, Sweden

Abstract

This paper presents a study of Diesel fuel wall films made in a high-pressure/high-temperature spray rig with the purpose to characterize wall film formation from impinging sprays at different injection conditions and to investigate the applicability of different optical techniques. Sprays are impinging on a quartz surface and the formed fuel film is illuminated by laser light through the quartz and the induced fluorescence is imaged from below. The illumination and detection is either done with a combination of a continuous laser and a high-speed video camera or with a pulsed laser and an intensified CCD camera. The first configuration enables following the development of individual sprays and allows for rapid data collection, whereas the latter provides snapshot images with a higher signal-to-noise ratio. The air density, varied by changing temperature or pressure, has an influence of the velocity of the spray arriving at the surface, but found to have less influence on the velocity of the leading edge of the fuel film propagating on the wall. When the air and wall temperature is raised above 200°C the film propagation velocity and the fuel film area are reduced due to fuel evaporation. When the fuel injection is split into several consecutive pulses, a reduction in film thickness and as well as film area is seen at the end of each pulse, followed by a rapid increase at the start of the following pulse.

Introduction

Background

Wall wetting can for different injection strategies and engine specifications occur in both spark-ignited (SI) and compression-ignited (CI) direct-injected (DI) engines and might affect the mixture formation and combustion with poor efficiency and increased pollutant emissions as a result. Particularly in DI Diesel engines, sprays can reach the walls of the combustion chamber both in small bore engines, where the distance between the injector hole and the walls is small, and in large unit displacement engines, in which a considerable amount of fuel is usually injected at each cycle. One way to improve the efficiency of SI engines is to apply direct injection of the fuel, which give advantages both in homogeneous and stratified operation mode, but the risk of fuel deposition on the piston or other surfaces in the cylinder makes it difficult to meet future more stringent regulations on particle emissions.

Furthermore, in for example homogeneous charge compression-ignition (HCCI) engines, the fuel can be injected early during the intake stroke, where the spray penetrates far into the cylinder and evaporates moderately. The in-cylinder walls or the piston can be wetted by the fuel. Another example is when injecting the fuel shortly after intake valve closing, the in-cylinder air temperature and density are low so that the spray can penetrate a long distance even though there is a lengthy time for mixing in non-evaporating conditions.

For these examples of direct injected Diesel, HCCI and SI engines, the investigation of impinging sprays and liquid wall film development is fundamental in order to predict its influence on the mixture formation. Moreover, simulations of these phenomena for fuel sprays need to be validated and improved; nevertheless they can extend and complement experimental measurements. In fact, heat transfer is significantly affected by the wall film thickness.

Motivation and objectives

Several studies about wall films have been conducted in the past, but nevertheless, there is not yet a real basis of knowledge in the field. Numerical simulations and experimental studies of spray/wall interaction have been done at Chalmers [1] and it has been found that a method for measuring the fuel wall film of impinging sprays is needed for validation.

*Corresponding author: alfhugo@chalmers.se

Optical methods can be used to investigate wall film formation, including film extension and thickness. Laser-induced fluorescence (LIF) is a powerful and versatile technique for the imaging of fuel distribution by illuminating fuel containing fluorescent molecules with laser light and detect the induced fluorescence with a camera. From the image the film area can be determined and the fluorescence intensity is a measure of the film thickness. A particular challenge is to obtain an efficient illumination of the wall film without inducing or detecting fluorescence from fuel drops or fuel vapor.

This can be achieved by using an optically transparent wall material such as quartz and illuminating the fuel film from inside the quartz with an incidence angle of the light that is large enough to ensure total internal reflection at the quartz-air interface, but not larger than that the laser light can penetrate into a fuel film which has a refractive index more close to quartz than to air. This approach has been applied in engines by Kull et al. [2] and by Cho and Min [3] as well as in spray chamber experiments by Alonso et al. [4]. An alternative approach for LIF is illumination and light detection through optical fibres [5, 6, 7]. The application of optical fibres limits the measurement to single points, but in these points data can be continuously recorded by photomultipliers.

Fuel films can also be characterized by the refractive index matching (RIM) method [8]. In the RIM method the film is formed on a glass or quartz surface with a micro-scale roughness, which efficiently scatters light. However, if the surface is wetted with a liquid with a refractive index relatively close to that of the wall material the scattering efficiency is reduced due to the smoother liquid air interface. Thus, the detected amount of backscattered light is reduced with increasing film thickness.

In this study fuel films formed by a Diesel fuel spray impinging on a quartz surface in a spray chamber are characterized by the LIF method with imaging. The method is applied both with a pulsed laser and an intensified CCD camera and with a continuous laser in combination with a high-speed video camera. The film formation at different fuel injection conditions such as fuel pressure, air pressure and temperature was investigated.

Experimental setup

The experimental study was made in the High–Pressure/High–Temperature (HP/HT) spray rig at Chalmers, Fig. 1a. It consists of a spray chamber with optical access, a fuel system, data acquisition and control systems together with an optical system suitable for spray diagnostics. The spray chamber consists of two cylindrical shells: an outer shell of thick steel to withstand the air pressure and a thin inner liner to give a thermalized measurement volume of approximately 1.5 dm^3 for this configuration, Fig. 1b.

The air in the spray chamber is delivered from a Hamworthy 4-cylinder (4-stage) compressor of 400 bar, continuously delivering pressure up to 100 bar. The pressurized air is then heated to a maximum of 625°C with two heaters placed at the inlet of the chamber and a surface heater close to the injector. The experimental conditions are determined by controlling the air flow and temperature. The air flow is kept low to achieve quiescent conditions but also sufficiently high to cool the heaters and refresh the atmosphere in the chamber between injections. The four windows used for optical access have a visibility area of approximately 45x110 mm^2 each and allow the laser light to enter at an appropriate angle.

The fuel spray is generated by a common-rail injection system with a solenoid injector equipped with a single-hole nozzle. The fuel pressure, the number of injection pulses and the length of each pulse are parameters that can be varied. The time between fuel injections is typically 5 to 10 s to allow the conditions in the camber to stabilize after the previous injection.

The wall design

The wall, shown in Fig. 1c, consists of several metal parts and a quartz piece, and has a flat top surface with a diameter of 52 mm. The distance between the wall, which is mounted from the bottom of the chamber, and the injector, which is mounted in the top of the chamber can be varied from less than 20 mm to more than 60 mm. To enable laser illumination and imaging a part of the wall consists of a rectangular piece of quartz, 42x21x15 mm. It rests on an O-ring seal and is placed over an opening in the metal structure allowing a rectangular area of 34x15 mm of the surface, onto which the fuel spray impinges, to be viewed from the bottom of the chamber. The laser light enters and exits through the smaller surfaces, and is by a prism mounted on the side of the wall directed into the quartz piece at an angle of approximately 40 degrees to the surface normal, making the incidence angle of the light at the upper surface approximately 65 degrees. At this angle the light would be transmitted into a fuel film on top of the quartz piece, but is totally reflected at a planar quartz-air or fuel-air interface. The wall is designed to operate at pressures up to 100 bar, and temperatures of at least 325°C. In this experiment it was used at up to 30 bar and 300°C. The temperature of the wall cannot in the present configuration be controlled independently, but the surface of the wall is assumed to reach the same temperature as the air inside the chamber.

The optical set-up

The excitation and detection was carried out with two different combinations of lasers and cameras, Fig. 1c. In the first configuration an argon-ion laser, continuously emitting light at the wavelengths of 488 and 514 nm, was used for excitation. The light beam was expanded to a diameter of 15 mm before entering the spray chamber through one of the large side windows. The quartz prism mounted on the side of the wall directed the light into the rectangular quartz piece, where it illuminated an oval area with long and short axes of approximately 30 and 15 mm respectively. Fluorescence light was detected through the bottom of the chamber where a mirror directed it towards a high-speed video (HSV) camera with an image intensifier. A long-pass filter was placed in front of the camera to remove scattered laser light. Images were typically recorded at a rate of 10000 images per second. In the other configuration the third harmonic light at a wavelength of 355 nm from a pulsed Nd:YAG laser was used for excitation and an intensified CCD camera was used for the detection of the fluorescence light. Otherwise the optical set-up was practically identical. Since the repetition rate of the Nd:YAG-laser was 10 Hz, only one image per injection could be recorded, and to be able to follow the time evolution images were recorded at different times after start of injection.

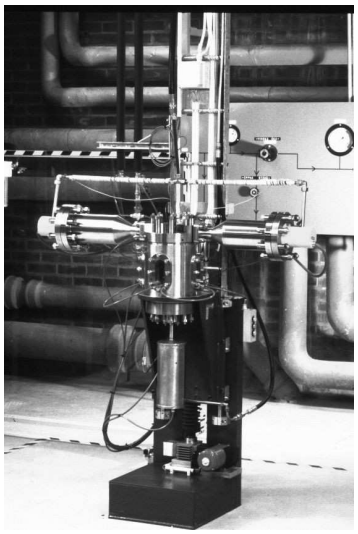

(a) Photo of the spray rig with the spray chamber located in the middle together with air heaters and pipes

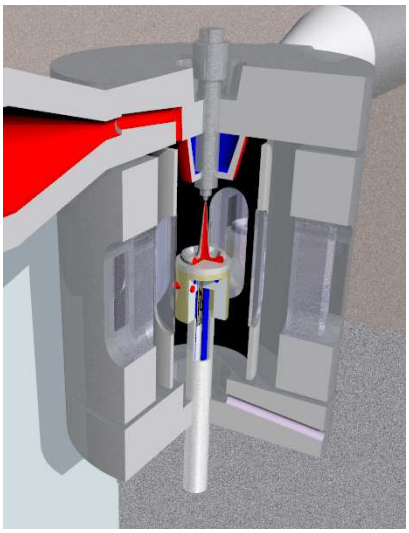

(b) Sketch of the spray chamber with a four-window configuration demonstrating a height adjustable wall

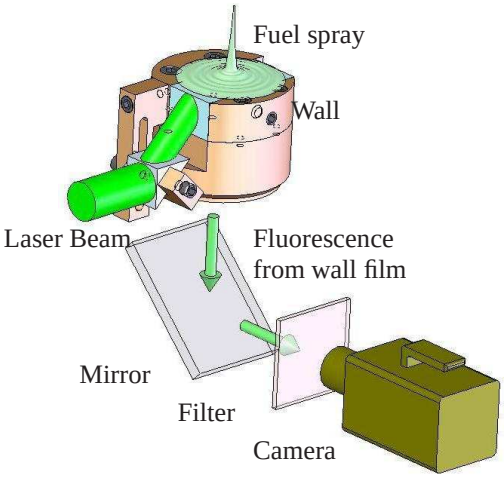

(c) Sketch of the optical setup for the continuous laser with a mirror, a high-pass filter, and a high speed camera to record the fluorescence from the wall film

Figure 1. Photo (a) and drawing (b) of Chalmers' High-Pressure/High-Temperature spray rig, and drawing of the wall for fuel film measurements (c).

Fuel and tracer

The commercial Diesel fuel of Swedish Environmental Class 1 used in the experiment has a specific green color given by dye molecules, Solvent Yellow and Solvent Blue, added as labeling the fuel as low-tax fuel. The amount of tracer solved in the fuel should be at least 6 mg Solvent Yellow 124 per liter of fuel, and this tracer is selected in part because it is difficult to extract from the Diesel fuel. To increase the strength of the green fluorescence the concentration of Solvent Yellow 124 was in this experiment doubled to about 12 mg per liter.

The fluorescence yield is much higher when the fuel is excited by UV-light compared to excitation with blue or green light, and in addition there may be a contribution from other fluorescing compounds in the fuel. Excitation at a wavelength of 355 nm results in a broad emission between 370 and 550 nm with peaks at 380, 400, 425 and 460 nm and a tail stretching out into the red as can be seen in Figure 2. The absorption and thereby excitation efficiency is much lower at 488 nm and even lower at 514 nm, and a significant fluorescence is only detected at wavelengths longer than the excitation wavelengths. Peaks in the fluorescence spectra appear at 530 and 560 nm for excitation at 488 and 514 nm respectively. The linearity of the fluorescence intensity as a function of film thickness was verified to thicknesses of at least 40 micrometers, by measuring the fluorescence from fuel films between the quartz piece and another quartz window placed on top of it with well-defined spacers in-between.

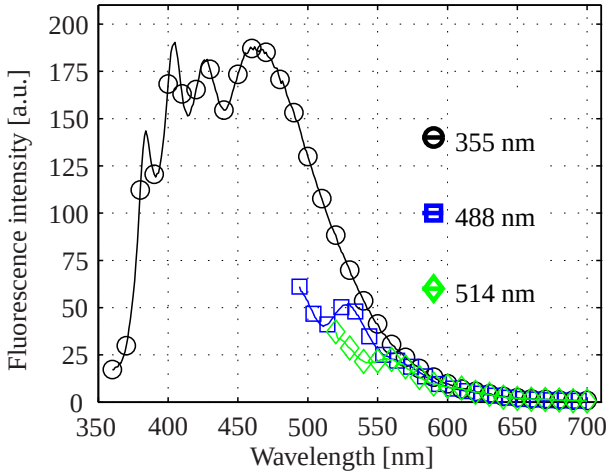

Figure 2. Fluorescence spectrum of the Diesel fuel.

Experimental parameters and analysis methods

To compare the two different techniques, a pulsed versus a continuous laser, and the other including parts of the equipment, the conditions inside the spray chamber where chosen to start at a rather low air temperature and air pressure. Both techniques where tested before increasing the air density and an example of the acquired images from the HSV and the intensified CCD cameras are shown in Figs. 3 and 4, respectively.

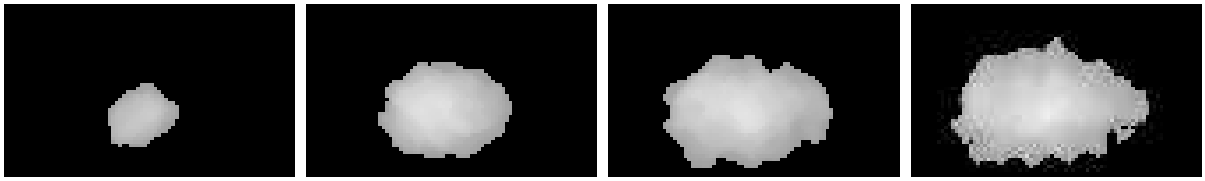

(a) Time after impingement = 100μs | (b) Time after impingement = 300μs | (c) Time after impingement = 500μs | (d) Time after impingement = 700μs

Figure 3. Processed pictures – Continues laser. Image area approximately 31x17 mm.

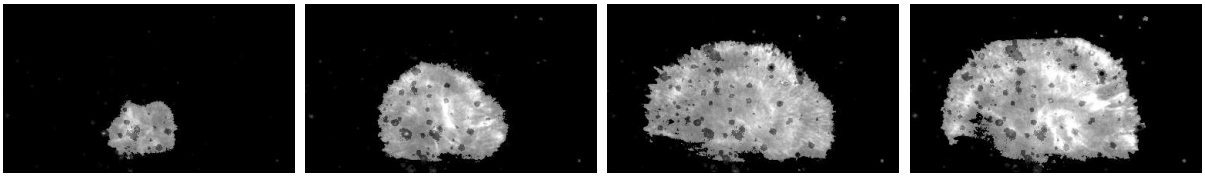

(a) Time after impingement = 100μs | (b) Time after impingement = 300μs | (c) Time after impingement = 500μs | (d) Time after impingement = 700μs

Figure 4. Unprocessed pictures – Pulsed laser. Image area approximately 31x17 mm.

One parameter of interest is the propagation of the film on the wall and to quantify this, the diameter of the film is measured from images of subsequent time steps. Two limitations have to be considered though, firstly the visible area of the glass and secondly the area of the incoming laser beam which illuminates the surface of the quartz glass. This gives a visible illuminated area of between 200 and 350 mm^2, depending on the size of the laser beam, as shown in Fig. 5a. Due to stochastic variations in the spray behavior the center of the wetted area is not exactly aligned with the nozzle tip center, Fig. 5b. Since the leading edge of the film more quickly reaches the edge of the illuminated area in some directions, e.g. downwards in the image shown in Fig. 5a, the film extension is measured along the longer axis of the quartz piece, as shown in Fig. 5b. To calculate the diameter, first the background intensity, determined from images recorded before the spray impinges, is subtracted and then the intensity in the images below a threshold value is set to zero.

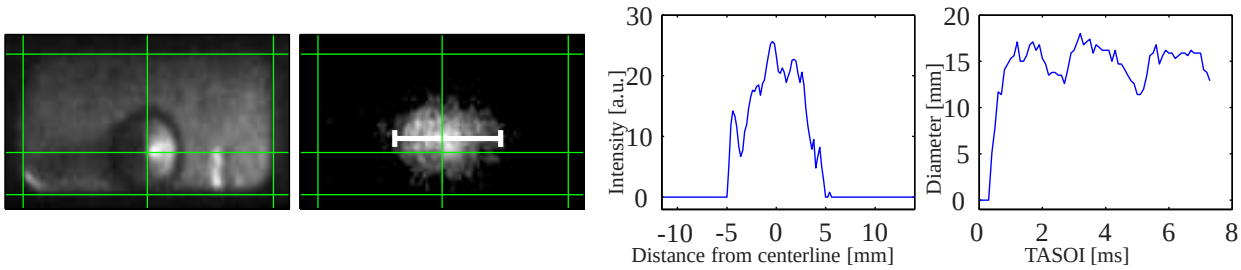

(a) Visible area and the nozzle tip center

(b) Approximated diameter of fuel film

(c) Intensity of 5 averaged rows

(d) Averaged diameter after start of injection

Figure 5. Definition of fuel film spreading

Thereafter an average of several pixel rows at the center of the footprint of the spray is extracted for each image. From these intensity profiles, an example shown in Fig. 5c, the width of the fuel film in one direction can be determined, with the white bar in Fig. 5b indicating the diameter. Using this procedure the film diameter is determined for each time step and an example of the evolution as a function of time is shown in Fig. 5d.

Results

Different parameters were studied, such as evolution of film area/diameter from which film velocity can be derived and intensity which is a measure of thickness. The influence of different conditions like, injection strategy, injection pressure, distance to the nozzle, air pressure and air temperature was investigated. To demonstrate and compare the capability of the two illumination and detection schemes the diameter of the footprint from the impinging spray was measured at identical conditions. As can be seen in Fig. 6 the increase in diameter is similar up to 15 mm. The different behavior after 15 mm can be explained by different diameters and intensity profiles of the laser beams, as well as by the fact that the edge is less sharp using the HSV camera due to the film edge propagating during the exposure time and a lower signal-to-noise ratio. The different exposure times of the two cameras also influences the determination of the time-of-impingement and is, thus, responsible of the small shift between the curves in Fig. 6. It can also be noticed that the diameter from the pulsed laser set-up is calculated from 5 different sprays at each time step, thus more sensitive to spray-to-spray fluctuations and variations in conditions with time while the diameter from the continuous laser set-up is calculated by following the development of 5 sprays.

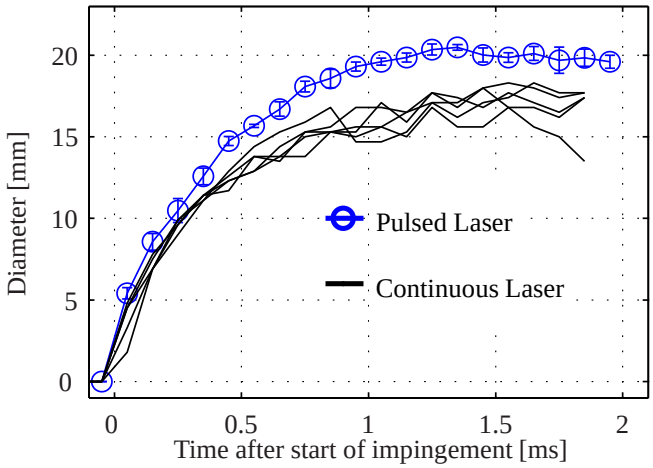

Figure 6. Calculated diameter from both the continuous and pulsed laser. T_{air} = 200 °C p_{air} = 5.5 bar. Injection pressure = 1350 bar and distance to the wall = 60 mm.

An investigation of the influence of the air temperature on the wall film spreading can be seen in Fig. 7. It can be noticed that the film starts to form somewhat earlier at the highest temperature, which indicates that the time from the opening of the injector to the arrival of the fuel at the wall is shorter due to the lower air density which influences the aerodynamic drag. However, the velocity of the leading edge of the fuel film on the wall is not higher at 200°C, compared to the lower temperatures, and 0.6 ms after the first impingement the diameter is almost the same for all three temperatures. The smaller maximum diameter at 100°C is due to a smaller illuminated area.

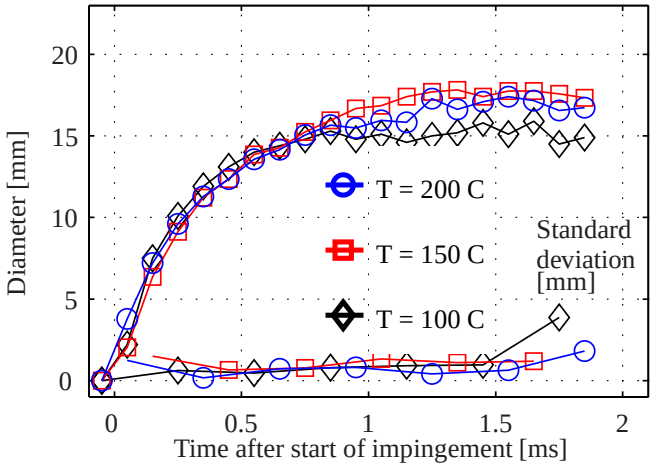

Figure 7. Calculated diameter from the continuous laser. T_{air} = 100, 150 and 200 °C, p_{air} = 5.5 bar. Injection pressure = 1350 bar and distance to the wall = 60 mm.

Similar trends can be seen in Fig. 8, based on ICCD-images taken at a shorter nozzle-wall distance. At the higher temperature the first liquid fuel arrives earlier, but the film propagation is not faster. Actually, after 0.5 ms the film propagates more slowly at the higher temperature and the maximum diameter is smaller at 250°C. This is likely an effect of that fuel evaporation becomes significant on the millisecond time scale above 200°C.

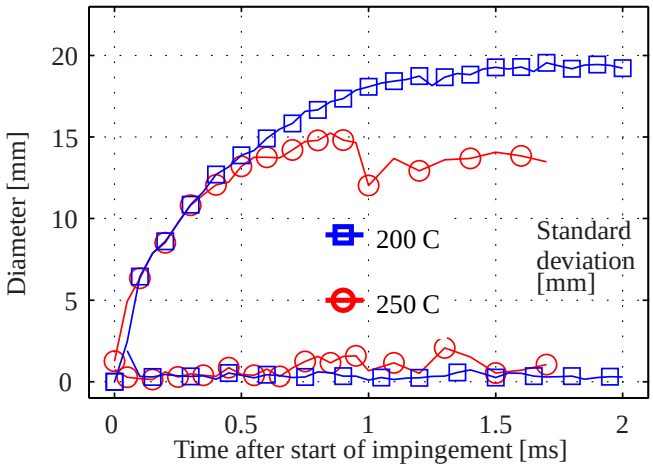

Figure 8. Calculated diameter of the impinged fuel from the case with a pulsed laser. T_{air} = 200 and 250 °C, p_{air} = 5.5 bar. Injection pressure = 1350 bar and distance to the nozzle = 45 mm.

An increase in air pressure enhances the differences in the fuel film evolution measured at different temperatures as can be seen in Fig. 9, showing film diameters measured at an air pressure of 10 bar. During the first 0.2 ms the increase in film diameter is relatively similar for the three air temperatures applied. Thereafter, the film evolution at 200°C is similar to that at 5.5 bar, whereas the increase in film diameter becomes significantly slower at 250°C and at 300°C the diameter remains constant at approximately 6 mm after 0.2 ms after the first fuel impingement. At a higher air pressure the heat transfer to the fuel drops in the spray is more efficient and more fuel is expected to have evaporated already before the liquid drops arrive at the wall, and the evaporation from the wall is also expected to become more rapid. Thus, at 10 bar and 300°C steady-state-like conditions appear to have established shortly after the fuel reached the wall, with a constant liquid area as long as liquid fuel is supplied from spray, but a rapid disappearance of the fuel film thereafter.

At a constant temperature of 200°C, the main influence of changing the air pressure is a delay of the arrival of the spray to the surface of the wall due to the higher air density, as can be seen ing Fig.10. Note that in Fig.10 the time scale is with reference to the start of impingement of the 10-bar case to demonstrate the difference in arrival times. The lower velocity of the spray arriving at the surface does not automatically translate to a slower propagation of the fuel film on the quartz surface, since the initial increase in film diameter is comparable for 10, 15 and 20 bar. Even if the axial velocity of the fuel drops arriving at the surface is different for the different cases, the fuel mass arrival rate is approximately the same at the different pressures. However, at 25 bar not only the film propagation speed is lower also the maximum film diameter is smaller. This might be caused by an increasing evaporation due to longer and stronger interaction with the surrounding air leading to a larger fraction of the fuel having evaporated before arriving to the surface. Furthermore, the higher pressure could affect spray characteristics such as drop size and spray angle, also influencing the evaporation and/or the footprint of the spray.

The evolution of the fuel film when the fuel injection was split into three pulses was investigated. Each injection was 1.5 ms long with a 1.0 ms dwell between the injections. The evolution of the film diameter and the total fluorescence intensity at an air temperature of 200°C and pressure of 5 bar is shown in Fig. 11. The film evolution during the first of the three pulses is as expected similar to that of a single pulse. After the end of the first pulse, when fuel stops arriving at the wall, there is rapid decrease in the total fluorescence intensity and also the measured diameter decreases. In about 0.3 ms the fluorescence intensity drops to less than half of the value during the injection and the reduction decreases also after that but at a reduced rate. There is also a reduction in the measured film diameter of a few millimeters during the dwell. The rapid reduction in fluorescence intensity shows that the film thickness decreases during the dwell, although an increased temperature of the diesel fuel also contributes to a lower fluorescence intensity.

When the fuel from the second injection arrives at the wall, the increase in fluorescence intensity is very rapid, quickly reaching same value as was observed at the end of the first pulse. Also the film diameter rapidly reaches the same value as at the end of the first injection, i.e. filling the maximum viewable area. The much more rapid increase in the fluorescence intensity and diameter during the second injection is likely due to that the fuel arrives at an already wetted surface and there is less resistance for the fuel to spread. Another factor that can contribute is that the spray of the second injection goes into the wake of the first one and, thus, the width of the spray and the footprint on the wall may be different. The reduction of the fluorescence intensity and the film diameter after the second injection is similar to that after the first one, and the film evolution during the third injection is practically identical to that during the second one.

Furthermore, the fluorescence intensity and film diameter during a triple injection at two different temperatures was compared. Figure 12 shows as a function of time the averaged fluorescence intensity of five pixel rows along a line at the center of the footprint of the impinging fuel spray captured with the high speed camera and assembled as lines in a matrix. The right side figure shows in more detail the information that is summarized in Fig. 11. After the fuel of the first injection arrives, it is possible to follow how the film diameter grows, rapidly in the beginning and more slowly afterwards. It can be noted that the fluorescence intensity of the film-covered areas is almost constant during the injection, and that the growth in total fluorescence intensity vs time, as seen in Fig. 11, comes from a growing film area. After the end of the first injection the drop in fluorescence intensity occurs almost instantaneously all over the film area, and the intensity in the outer parts of the illuminated film area drops under the threshold resulting in a smaller film diameter. Upon the arrival of the second injection, the fluorescence intensity quickly recovers over the whole film area almost instantaneously reaching the same level as during the first pulse. The general development of the film, including the behavior during and between the injection pulses, is similar at the two temperatures. The main difference is a higher fluorescence intensity and a higher maximum film diameter at 150°C.

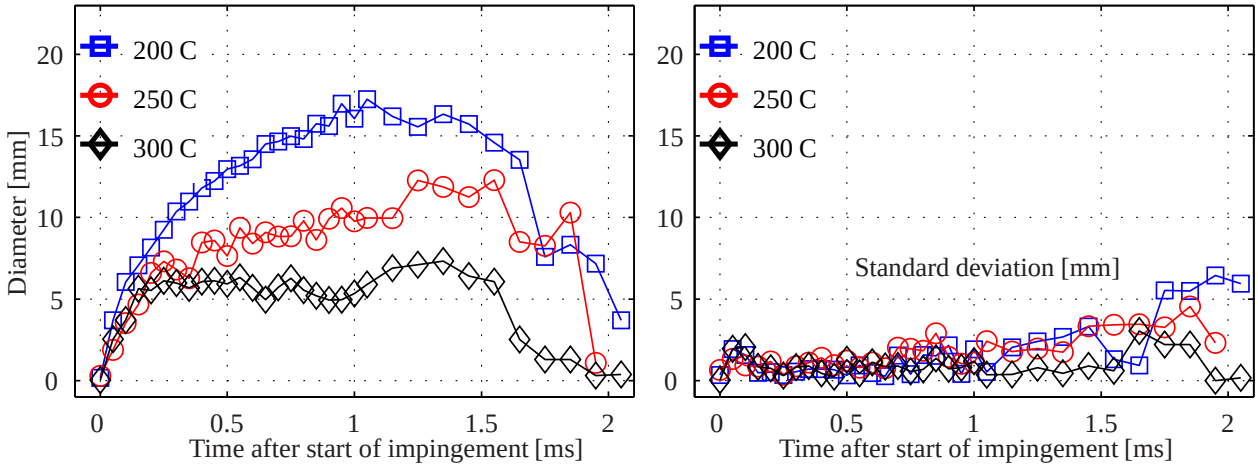

Figure 9. Calculated diameter of the impinged fuel from the case with a pulsed laser. T_{air} = 200, 250 and 300 °C, p_{air} = 10 bar. Injection pressure = 1350 bar and distance to the wall = 45 mm.

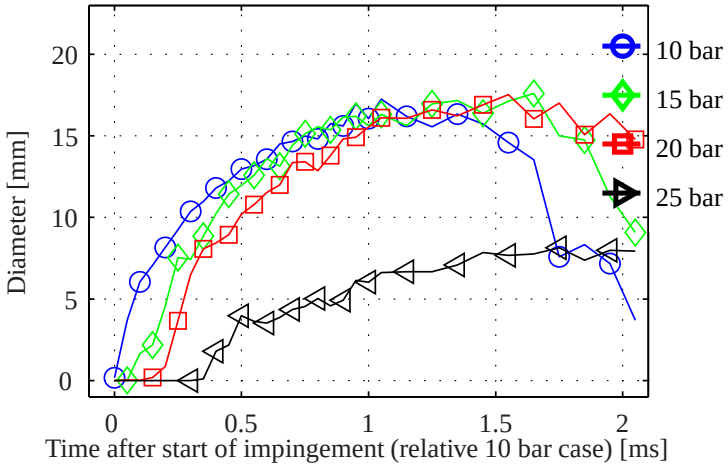

Figure 10. Calculated diameter of the impinging spray from the case with pulsed laser. T_{air} = 200, °C p_{air} = 10, 15, 20 and 25 bar. Injection pressure = 1350 bar and distance to the wall = 45 mm.

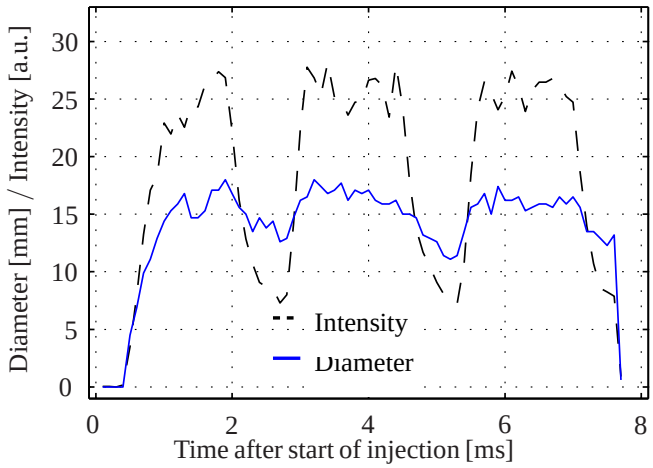

Figure 11. Calculated diameter and integrated intensity of the impinging spray from the case with continuous laser. T_{air} = 200 °C p_{air} = 5 bar. Injection pressure = 1350 bar and distance to the wall = 60 mm.

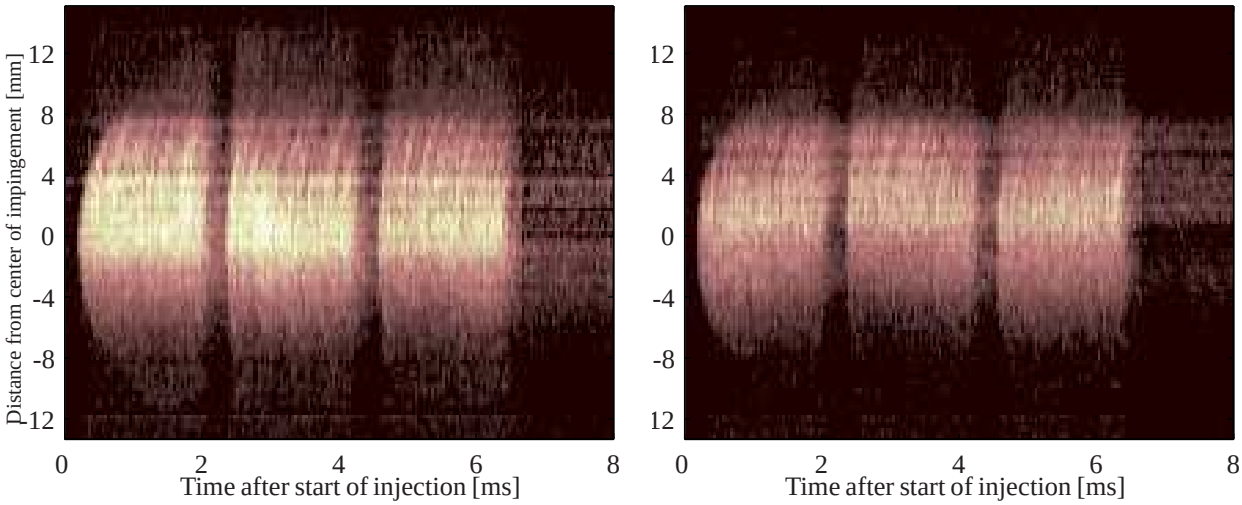

Figure 12. Averaged fluorescence intensity of five pixel rows at the center of the footprint of the spray merged into one matrix for each test case. Background subtraction were made without any filtering. The continuous laser was used for illumination. T_{air} = 150 and 200 °C p_{air} = 5.5 bar. Injection pressure = 1350 bar and, distance to the wall = 60 mm.

Conclusions

The use of pulsed and continuous lasers was compared and each concept was found to have its advantages, although it should be stated that information on film properties, such as film propagation speed and relative film thickness, determined with the two methods agree within expectations. The continuous laser combined with a high-speed video camera, makes it possible to follow the complete evolution of individual sprays time step by time step without having to compare images from different injection cycles. This possibility to record the full time sequence from an individual spray reduces the total measurement time significantly, which also minimizes the problem of fuel residuals building up a permanent film on the quartz surface during the measurements.

The excitation by light from the pulsed UV-laser provides images with a much higher signal-to-noise ratio, in part due to the much higher light intensity during the laser pulse and in part due to the higher fluorescence yield upon excitation with UV-light. The images recorded by pulsed laser illumination can be regarded as snap-shot images showing the fuel distribution at a particular moment with internal structures in the fuel film visible, while the images recorded by the video camera are averages during the typical exposure time of up to hundred microseconds.

The evolution of the film, and in particular the film diameter, was investigated as a function of several parameters such as air pressure and temperature, and injection sequence. The dependence of the different parameters is partly coupled, for example changing the air density either by changing pressure or temperature leads to a lower spray velocity and later arrival of the spray to the wall, but no corresponding change in the film propagation rate on the wall was noticed. When the temperature is raised above 200°C the extension of the wall film decreases, due to evaporation of the fuel. When the spray was split into a sequence of injection pulses a rapid decrease in the film thickness and diameter could be observed at the end of each injection pulse. When the fuel from the next pulse arrived at the wall the increase in film thickness and diameter was much faster than during the first injection pulse, likely due to the wall surface already being wetted.

Acknowledgements

Financial support from the Swedish Energy Agency and the Combustion Engine Research Centre (CERC) at Chalmers is gratefully acknowledged.

References

[1] A. Magnusson, *"Spray-Wall Interaction of Diesel Sprays"*, Ph.D. thesis, Chalmers University of Technology, 2009.

[2] E. Kull, G. Wiltafsky, W. Stolz, K.D. Min, E. Holder, *"Two-Dimensional visualization of liquid layers on transparent walls"* Optics Letters, 22, 645-647. 1997.

[3] C. Hoon, and K. Min, *"Measurement of liquid fuel film distribution on the cylinder liner of a spark ignition engine using the laser-induced fluorescence technique"*, Measurement Science and Technology, 14, 975-982, 2003.

[4] M. Alonso, P.J. Bowen, P.J. Kay, R. Gilchrist, S. Sapsford, *"Quantification of 3D transient fuel films for G-DI sprays under elevated ambient conditions"*, Proceedings of ILASS Europe 2008, Paper ID ILASS08-7-3, 2008.

[5] R. Lindgren, R. Block, and I. Denbratt, *"Development of a Wall Film Measuring Device"*, Proceedings of the 1^{st} International Conference on Optical and Laser Diagnostics (ICOLAD), London, 2002.

[6] S. Park, J.B. Ghandhi, *"Fuel Film Temperature and Thickness Measurements on the Piston Crown of a Direct-Injection Spark-Ignition Engine"*, SAE Paper 2005-01-0649, 2005.

[7] Y. Takahashi, Y. Nakase, H. Ichinose, *"Analysis of the Fuel Liquid Film Thickness of a Port Fuel Injection Engine"*, SAE Paper 2006-01-1060, 2006.

[8] M.C. Drake, T.D. Fansler, A.S. Solomon, G.A Szekely, Jr., *"Piston Fuel Films as a Source of Smoke and Hydrocarbon Emissions from a Wall-Controlled Spark-Ignited Direct-Injection Engine"*, SAE Paper 2003-01-0547, 2003.